Electronic supplementary information

A natural polymer-based hydrogel with shape controllability and high toughness and its application to efficient osteochondral regeneration

Jueying Yang[a], Hui Wang[a], Weiting Huang[a], Kelin Peng[ab], Rui Shi[c], Wei Tian[c], Lizhi Lin[d], Jingjing Yuan[a], Weishang Yao[a], Xilan Ma[a] and Yu Chen*[ade]

[a] *School of Materials Science and Engineering, Beijing Institute of Technology, Beijing 100081, China.*

[b] *Yangtze Delta Region Academy of Beijing Institute of Technology, Jiaxing 314019, China.*

[c] *Beijing Research Institute of Traumatology and Orthopaedics, Beijing Jishuitan Hospital, Beijing 100035, China.*

[d] *Institute of Engineering Medicine, Beijing Institute of Technology, Beijing 10081, China.*

[e] *Sports & Medicine Integration Research Center (SMIRC), Capital University of Physical Education and Sports, Beijing 100191, China.*

* Corresponding author.
E-mail address: cylsy@163.com (Y. Chen)

S1 Experimental methods

S1.1 Materials

Chitosan (degree of deacetylation 90%) was purchased from Zhejiang Aoxing Biotechnology Co., Ltd. (China). Agar (grey scale≤1.5%) and sodium alginate (viscosity 200±20 mPa·s) was obtained from Shanghai Aladdin Industrial Corporation Co., Ltd. (China). Glycerol (content≥99.0%) was purchased from Sinopharm Chemical Reagent Co., Ltd. (China). Acetic acid (AR) and N,N-dimethylformamide (DMF) was obtained from Beijing Tongguang Fine Chemical Company (China). Calcium carbonate ($CaCO_3$) (AR) was purchased from Tianjin Chemical Reagent Co., Ltd. (China). Fetal bovine serum (FBS), the α-minimum essential medium (α-MEM), phosphate-balanced saline (PBS), trypsin, and penicillin/streptomycin were obtained from Gibco (USA). Live/dead cell double staining kit, cell counting kid-8 (CCK8), rhodamine-labeled alkaline phosphatase (ALP), and Alizarin Red-S staining (ARS) were purchased from Solarbio (China). Rat bone marrow mesenchymal stem cells (rBMSCS) were obtained from Cyagen Biosciences (Suzhou) Inc.

S1.2 Preparation of preformed hydrogel

Firstly, 1 wt.% Agar was added into a flask with a certain amount of deionized water and heated to above 100 °C to fully dissolve. After cooling to 50 °C, different weights of SA powders were slowly added to the above agar solution and stirred to dissolve completely. Secondly, CTS, $CaCO_3$ powders, and glycerol at different concentrations were added to the above solution and stirred for 2 h to form a uniformly viscous polymer sol. The sol was cast to form preformed hydrogels in an ambient environment below 35 °C for follow-up experiments.

S1.3 Preparation of hydrogels based on the PFDEPE method

After the preformed hydrogel was placed in a deep container, 50 mL 2% low-concentration acetic acid solution was poured over the preformed hydrogel to ensure the hydrogel was completely submerged in the solution to proceed with acidification dual-effect post-enhancing process until the hydrogel becomes transparent. The PEMN hydrogel with the post-enhancing process was then taken out and rinsed with water to remove the acetic acid on the surface, and sealed in valve bags before use. The PEMN hydrogels were labeled as PEMN-2.7%, 3.6%, 4.5%, 5.4%, and 6.3% according to different polymer ratios contained in the system. Different polymer ASC (Agar/SA/CTS) and ASCa (Agar/SA/CaCO3) hydrogels were prepared in the same way for comparison. SCCa and ASCCa hydrogels were prepared by the semi-dissolution

acidification sol-gel transition (SD-A-SGT) method for comparison. The different polymer contents and ratios of hydrogels are shown in Table S1.

S1.4 Preparation of hydrogels based on the SD-A-SGT method

SCCa hydrogels used for comparison could not be prepared by the PFDEPE method due to the absence of agar but were prepared by the SD-A-SGT method. Briefly, a certain mass of SA powders was slowly added to the deionized water and stirred to completely dissolve SA. Then, CTS, $CaCO_3$ powders, and glycerol were added to the above solution at different concentrations and stirred for 2 h until uniformly dispersed to form a viscous polymer sol. After stopping stirring, pour the sol into a petri dish and place it in an airtight plastic box filled with 100 mL of acetic acid to undergo a sol-gel transition and obtain a composite hydrogel. After 24 h, the hydrogel was taken out and rinsed with water to remove the acetic acid on the surface of the hydrogel.

ASCCa hydrogel prepared by the SD-A-SGT method was used for comparison. Briefly, 1 wt.% Agar was added into a flask with a certain amount of deionized water and was heated to above 100 °C to fully dissolve. After cooled to 50 °C, different weights of SA powders were slowly added to the above agar solution and stirred to completely dissolve SA. Then, CTS, $CaCO_3$ powders, and glycerol were added to the above solution at different concentrations and stirred for 2 h until uniformly dispersed to form a viscous polymer sol. After stopping stirring, pour the hot sol directly into a petri dish and place it in an airtight plastic box filled with 100 mL of acetic acid to undergo a sol-gel transition and obtain a composite hydrogel. After 24 h, the hydrogel was taken out and rinsed with water to remove the acetic acid on the surface of the hydrogel.

The compositions of SCCa and ASCCa hydrogels are shown in Table S1.

S1.5 Materials characterizations

The inverted bottle method was used by taking out the sol from 50 °C and pouring it into a glass vial quickly. The time from pouring into the bottle until the hydrogel does not flow in the inverted vial is regarded as the time for the formation of the preformed hydrogel.

The rheological properties of the hydrogels were measured by a Physica MCR302 rheometer (Anton Parr, Austria) equipped with a parallel plate. The frequency test was performed with a fixed strain of 1%, a constant temperature of 25 °C, and an angular frequency change of 1-100 rad s^{-1} to measure the storage modulus (G′) and loss modulus (G″). The temperature scan of a sol was performed with a fixed strain of 1%, a fixed frequency of 1 Hz, and a temperature change of 80°C~25 °C with a rate of 1 °C s^{-1}. The rheological

recovery behavior of the hydrogel was performed with a fixed frequency of 1 Hz for 200 s at a strain of 1% and for 40 s at a strain of 100%. For the rheological property comparison under different temperatures, the frequency test was performed with a fixed strain of 1%, a constant temperature of 25 °C or 35 °C, and an angular frequency change of 1-100 rad s^{-1} to measure G′ and G″ of the PEMN-2.7% hydrogel.

The binding energy of the elements in the samples was characterized by PHI Quantera II (Ulvac-PHI, Japan), equipped with a 25 W, 15 kV monochromatized Al KRX ray source. A broad-spectrum was scanned in the range of 0-1100 eV with a pass energy of 280.00 eV and a step size of 1.00 eV. High-resolution energy spectra were collected with a pass energy of 26.00 eV and a step size of 0.025 eV. The results were fitted and analyzed by a nonlinear least-squares curve fitting program (MultiPak software). Before performing the characterization, the samples were dried in an oven, which caused the collapse of the pores in the hydrogel, resulting in the formation of a flat solid. This approach was adopted to ensure that the results obtained from XPS analysis are minimally affected by air.

Functional group changes of various hydrogels were characterized using a Bruker ALPHA II Attenuated Total Reflection Flourier Transformed Infrared (ATR-FTIR) spectrometer (Bruker, Germany). For SA, CTS, and Agar, powder samples were directly used for testing. For hydrogels and sols, samples were dried with a freeze-dryer for 48 h to remove water for testing. The test range was 4000-400 cm^{-1}, the resolution used in the experimental test is 4 cm^{-1}, and the number of scans was set to 32 times. For the acidification kinetics, the process of forming PEMN hydrogels from preformed hydrogels after adding acid was repeatedly scanned with deionized water as the background, the scanning range was 4000-600 cm^{-1}, the resolution was 8 cm^{-1}, the number of scans was 16 times, and a scan was performed every 20 s for a total of 25 times.

Post-enhancement kinetics were measured by forming preformed hydrogels in graduated glass tubes, filled with acetic acid solutions of different concentrations and sealed. The post-enhancement process was observed by the change of the hydrogel from opaque to transparent at intervals.

Mechanical tests were characterized by an Instron Universal Materials Testing Machine (Instron, USA). In the tensile test, hydrogels were cut into a dumbbell shape with a tensile rate of 100 mm min^{-1}. In the compression test, hydrogels were cut into a cylindrical shape with a compressive rate of 2 mm min^{-1}. Each group of samples was tested three times and the average data and the standard deviation were calculated. The tensile energy to break was calculated by the area of the stress-displacement curve. The loading-unloading cycle was performed with the loading/unloading rate of 20 mm min^{-1} and the maximum strain of

50% 50 times. For the mechanical property comparison under different temperatures, PEMN-2.7% hydrogels were cut into a dumbbell shape, heated under 25 °C or 35 °C for 1 h, and tested immediately after taking out the samples with a tensile rate of 100 mm min^{-1}.

The adhesion test was performed by applying the sol to the surface of the pigskin to form a preformed hydrogel and then acidified with 1% acetic acid. The maximum adhesion strength was measured as the maximum load (N) divided by the adhesion area, and the adhesion energy was the area enclosed by the adhesion stress-displacement curve. For bioadhesion between the hydrogel samples, PEMN-2.7% hydrogel was placed between two pieces of pigskin or directly contact with one piece of pigskin at 37 °C for 1 h. The adhesion performance was evaluated using the 180° peel test on the prepared samples.

The water content was measured by weighing freshly prepared hydrogels before and after being freeze-dried. The water content was calculated with the following formula:

$$Water \quad Content = \frac{W_w - W_d}{W_w} \times 100\% \tag{S1}$$

In the formula, W_w and W_d are the mass of the freshly prepared sample and the freeze-dried sample, respectively.

Swelling ratio was tested using freeze-drying different hydrogel samples. A certain mass of samples was weighed and immersed in deionized water or PBS at 37 °C. The swelling ratio after 24 h was taken as the equilibrium swelling ratio. The swelling ratio is calculated by the following formula:

$$\text{Swelling ratio} = \frac{W_s - W_d}{W_d} \times 100\% \tag{S2}$$

In the formula, W_s and W_d are the mass of the sample after water absorption and the mass of the freeze-dried sample before water absorption, respectively.

The morphology of hydrogels was characterized using a Phenom Pro SEM (Phenom-Scientific, China). The voltage was 5.0 kV. The hydrogels were cut into blocks, and the block samples were fixed on an aluminum tray with the cross-section facing up using a conductive double-sided tape, and then the gold layer was sprayed with a sputter coater. The EDS mapping was tested using a field emission SEM Regulus 8230 (Hitachi, Japan) with a voltage of 10 kV.

The contact angle of Agar, preformed hydrogels, and PEMN hydrogels were tested using an OCA25 video contact angle meter (Dataphysics, Germany).

S1.6. Degradation test

The hydrogels were placed in 20 mL of PBS, 2 μg mL^{-1} collagenase II in PBS, and 10 μg mL^{-1} lysozyme in PBS, and placed in a constant temperature shaker at 37 °C with a shaking rate of 80 rpm to simulate the motion of the animal body. The samples were taken out every 7 days and rinsed with deionized water to remove the adsorbed substances. The degradation rate was calculated with the following formula:

$$Degradation \quad Rate = \frac{W_b - W_a}{W_b} \times 100\% \tag{S3}$$

In the formula, W_b and W_a are the mass of the hydrogels freeze-dried before and after being placed in the degradation solution, respectively. SEM characterization was used to observe the morphology after degradation. The structure of the degraded samples was tested using ATR-FTIR. For the molecular weight after degradation, because the cross-linked structure of the hydrogel made it insoluble in the solvent, the molecular weight of the slightly soluble part in the solvent can be obtained for comparison. Briefly, 2 mg of freeze-dried PEMN hydrogel and hydrogel degraded by lysozyme and collagenase II solutions for 12 weeks were placed in 1.5 mL of N, N-dimethylformamide (DMF) solution. After sonication for 6 h, the supernatant was collected. DMF was used as the mobile phase, polystyrene was used as the standard sample, and HLC-8320GPC gel permeation chromatography (TOSOH, Japan) was used to measure the weight-average molecular weight (M_w) at room temperature.[1]

S1.7 Cell viability

For cell viability, the hydrogels were spread at the bottom of 96-well plates in advance, and 1×10^4 rBMSCs were inoculated on the hydrogels. The viability was detected by CCK-8 after 24 h and 72 h and calculated by the following formula:

$$Cell \quad Viability = \frac{A_s - A_b}{A_c - A_b} \times 100\% \tag{S4}$$

In the formula, A_s, A_b, and A_c are the absorbance of samples with cells, culture medium without cells, and culture medium with cells, respectively.

For cell distribution and state, 2×10^4 rBMSCs were inoculated on the spread hydrogel in 48-well plates, stained with Live/Dead reagent after 24 h, and observed by a fluorescence microscope Leica DMI8A (Leica, Germany) as described.

S1.8 Osteogenic differentiation of rBMSCs cells in vitro

The rBMSC cells were inoculated on hydrogel and cultured for 24 h. The medium was changed into α -mem osteogenic induction medium containing 50 μg mL^{-1} ascorbic acid, 10 mM monosodium glycerophosphate, and 100nM dexamethasone. The osteogenic differentiation medium was changed every 2 days. rBMSCs were inoculated on hydrogels and placed in 6-well plates for 7 and 14 days, respectively. The samples were fixed with PBS solution containing 4% formaldehyde for 30 min, stained with 0.1% ARS solution at 37℃ for 30 min, washed with PBS 3 times, and observed under an inverted microscope Leica DMI8A (Leica, Germany). After the water in the middle hole of the plate was drained, cetyl chloride was added, and the supernatant was absorbed by standing at room temperature for 30 min. The absorbance of the sample was measured at a wavelength of 562 nm by an ultraviolet spectrophotometer.

S1.9 In vivo implantation

All procedures for animal experiments were approved by the Animal Care Committee of Hebei Kangtai Medical Laboratory Services Co., Ltd. All experiments were conducted following the guidelines of the local Animal Welfare Committee. Male rats (n=18) weighing 260-280 g were divided into a blank control group, a PEMN group, and a hydrogel control group. Osteochondral defects with a diameter of 2 mm and depth of 3 mm were prepared with a drill in the middle of the right leg pulley of rats. After cleaning the defect with normal saline, hydrogels were implanted, then the wound was sutured and disinfected with iodophor. Six rats in each group were sacrificed at the 6th weeks and 12th weeks, and femoral samples were harvested and stored in 4% paraformaldehyde.

The femoral of rats were scanned at 70 kV, 200 μA, and 10 μm pixels using Bruker Skyscan 2211(Bruker, Germany). 3D images were reconstructed by micro-CT system software with a grayscale of 220. Bone regeneration was quantified by calculating the ratio of bone volume to tissue volume (BV/TV) and bone mineral density (BMD) as described.

The specimens were decalcified in 10% ethylenediaminetetraacetic acid (EDTA) solution at room temperature for 30 days, then paraffin encapsulated and cut into 5 μm sections for histological staining for morphological evaluation. H&E, MASSON, and SAPPH-O/Fast Green were performed on the samples according to conventional methods to evaluate the cartilage-specific characterization.

Immunohistochemical analysis was conducted to analyze the expression of Collagen II.

Laser confocal (Olympus, FV1000) was used for observation and imaging under a 4× microscope.

S2. Results

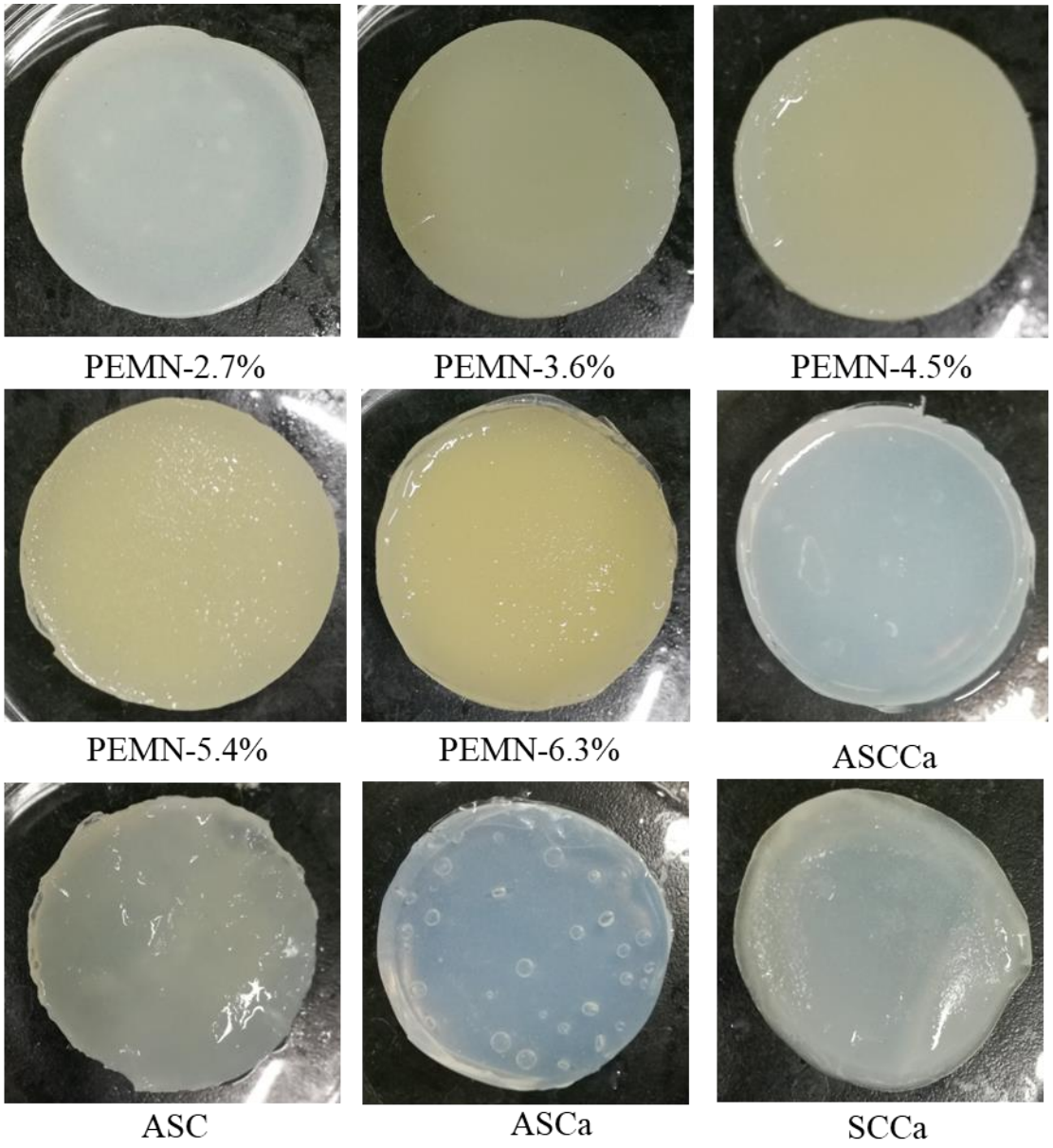

Fig S1. Appearance of hydrogels prepared by PFDEPE method or SD-A-SGT method with different components.

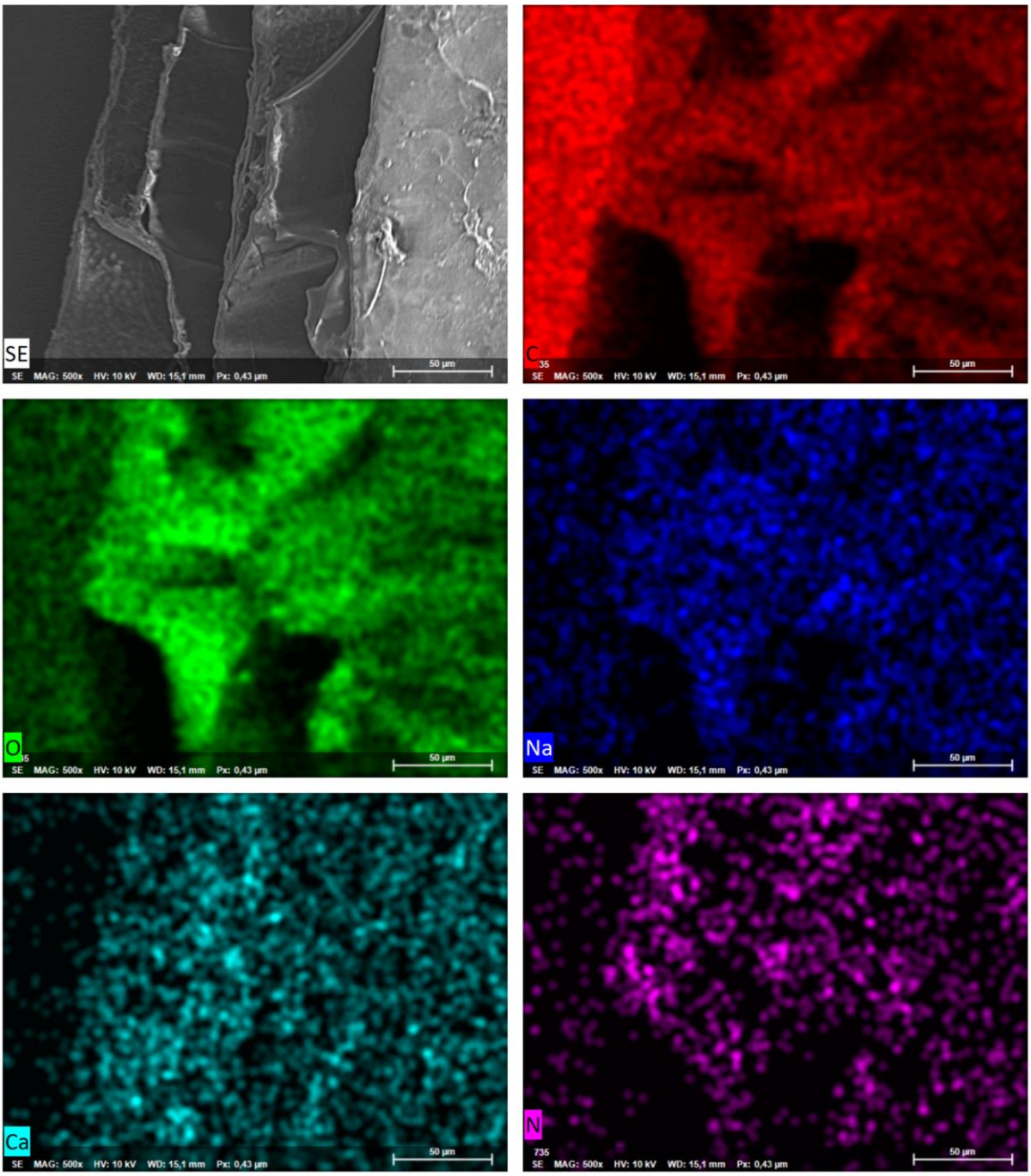

Fig S2. EDS analysis mapping of the PEMN hydrogel.

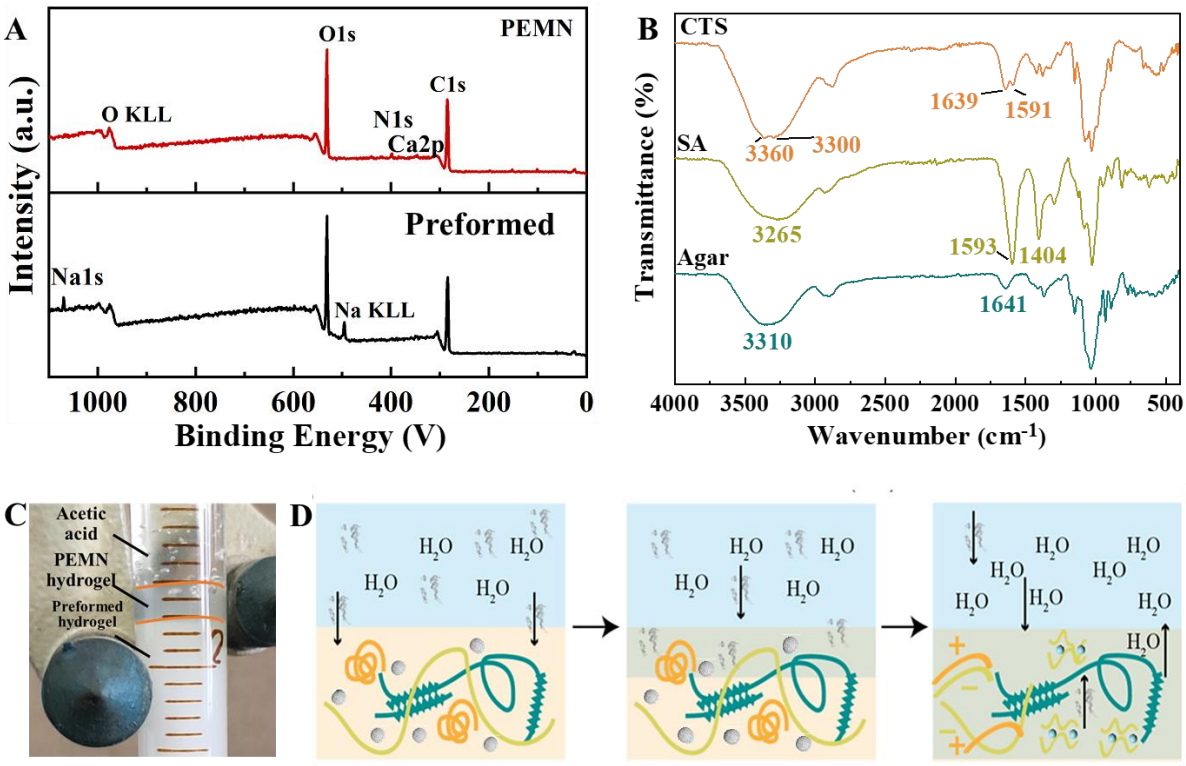

Fig S3. (A) Wide-scan spectra of XPS characterization results of preformed hydrogel and PEMN hydrogel. (B) ATR-FTIR results of Agar, CTS, and SA powders. (C) Transparent change of the preformed hydrogel and the PEMN hydrogel. (D) Schematic diagram of the speculative mechanism of post-enhancement.

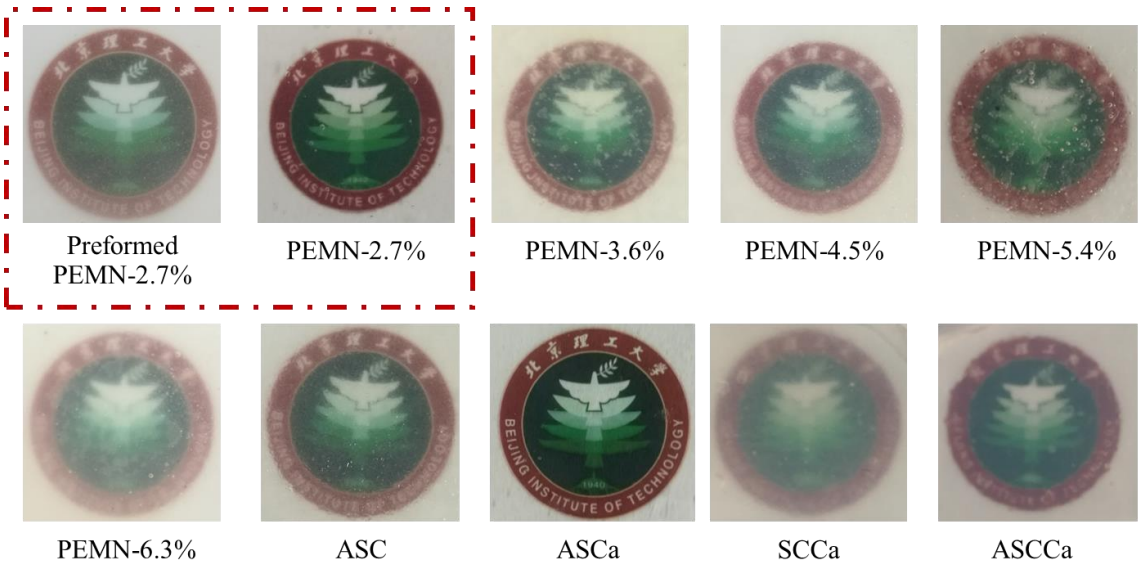

Fig. S4. The transparency of hydrogels prepared by PFDEPE method or SD-A-SGT method with different composition is different. The thickness of hydrogels is 2mm.

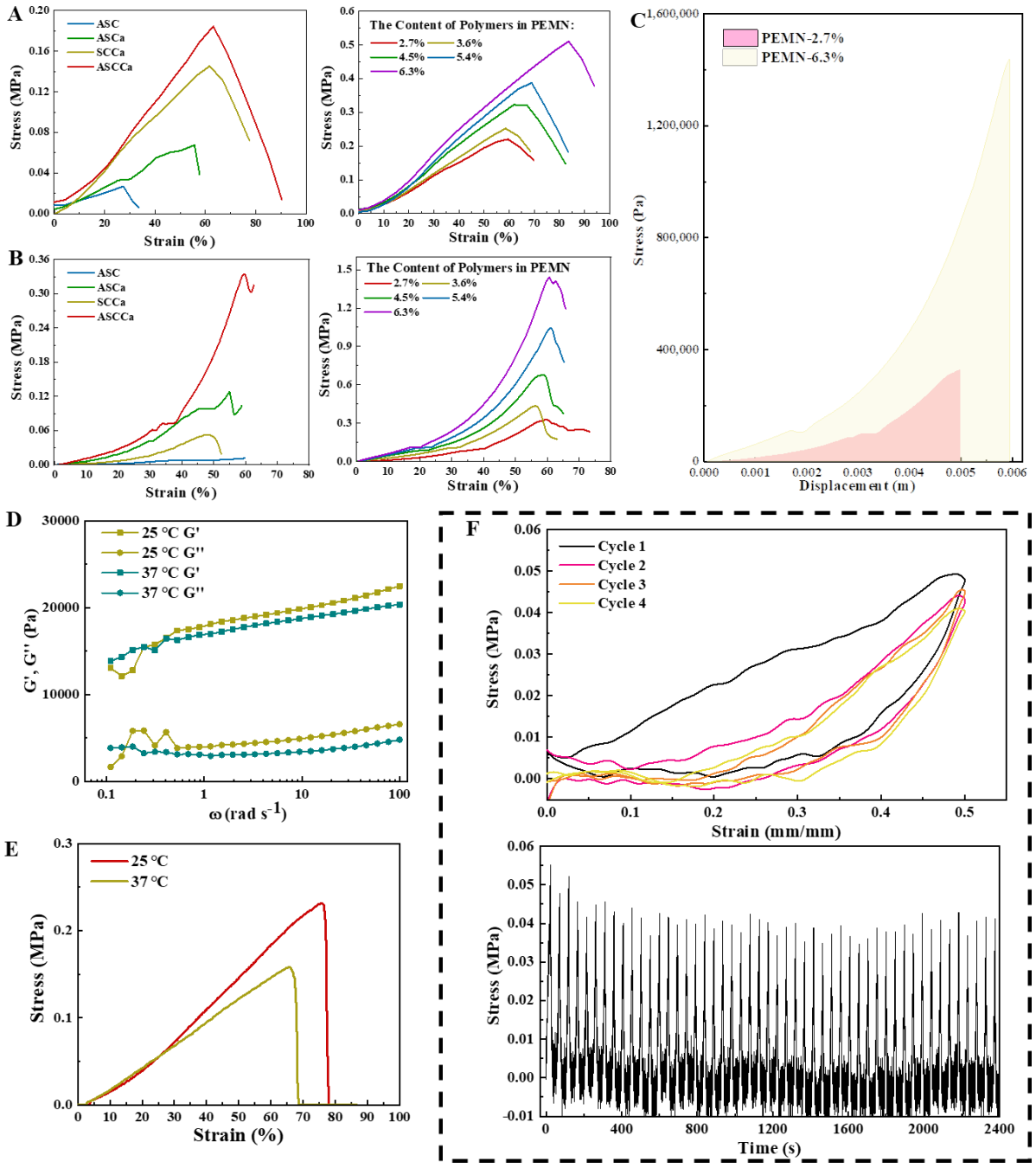

Fig. S5. Mechanical curves of hydrogels. (A) Tensile curve; (B) Compression curve. (C) Fracture energy calculation of compression curve for PEMN hydrogels with different ratios. (D) The rheological tests on the PEMN-2.7% hydrogel at 25 °C and 37 °C. (E) The mechanical tests on the PEMN-2.7% hydrogel at 25 °C and 37 °C. At 1% strain and 1 rad/s frequency, the storage modulus at 37 °C was 93.8% of that at 25 °C, indicating that the elastic properties did not differ significantly between these two temperatures. Furthermore, the results of the mechanical property tests showed that the tensile strengths at 37 °C and 25 °C were measured as 0.207 ± 0.035 MPa and 0.173 ± 0.021 MPa, respectively, with a relatively small difference. (F) Tensile cyclic curve of PEMN hydrogel.

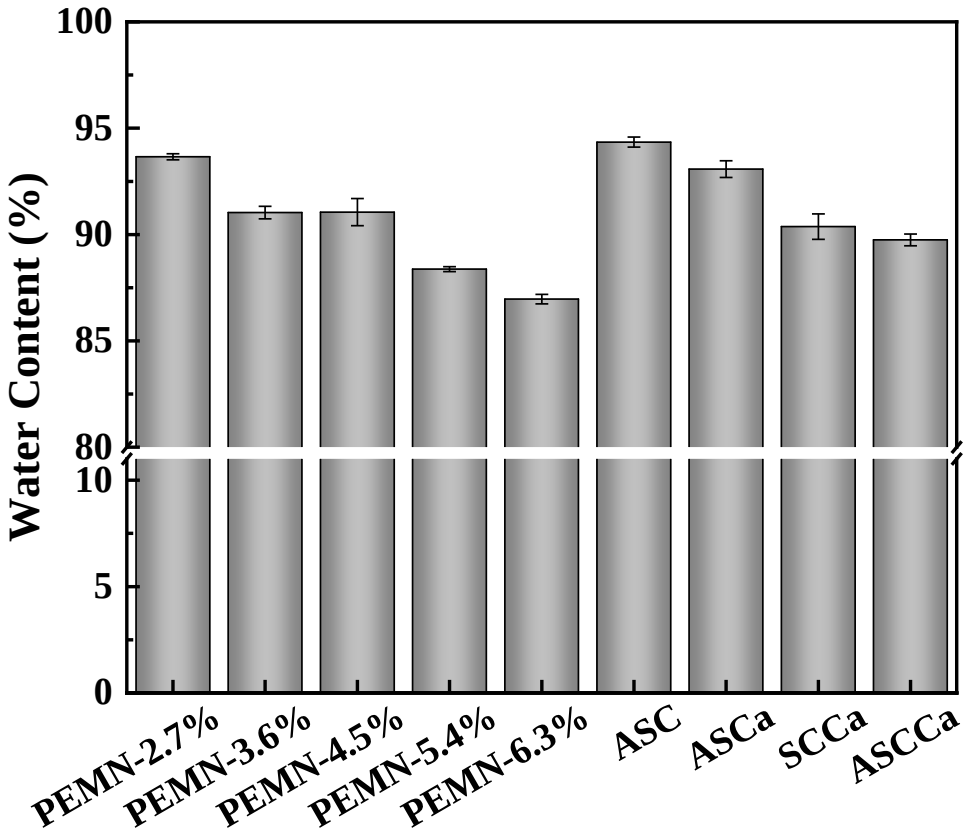

Fig. S6. Water content of hydrogels of different compositions.

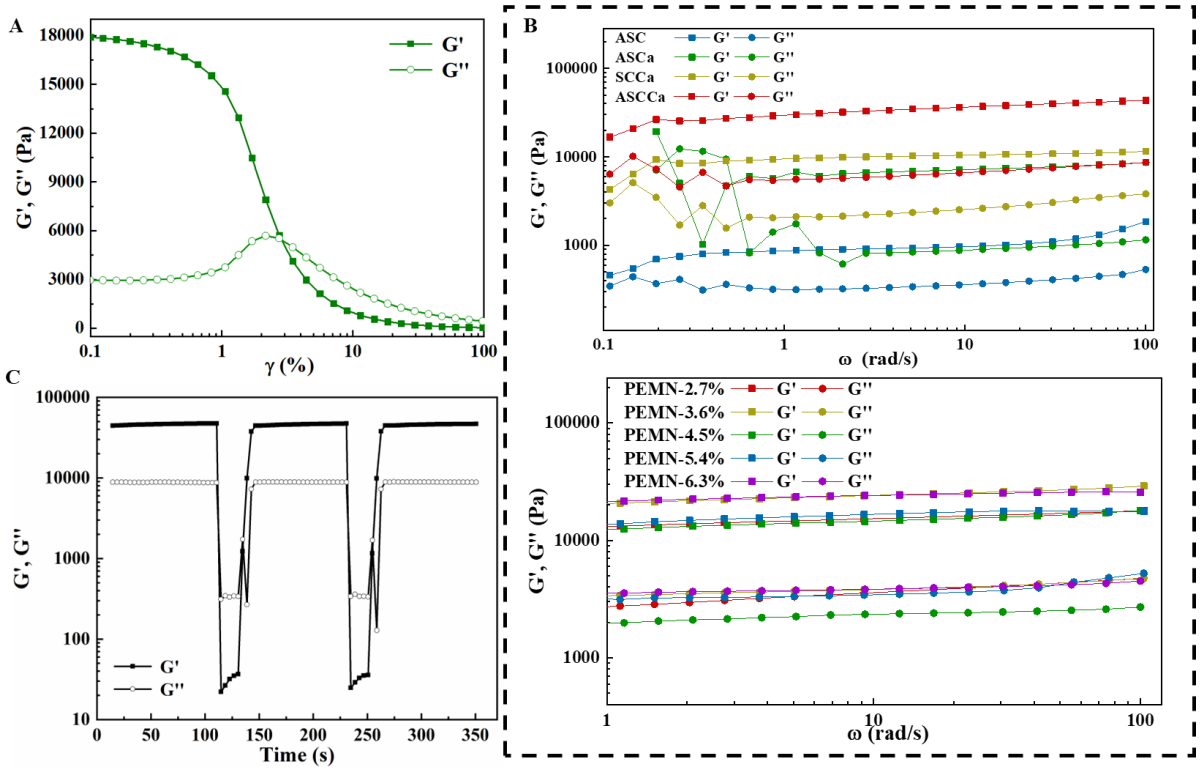

Fig. S7. Rheological results. (A) Rheological strain change results of the PEMN hydrogel (fixed stress 1Hz). The constant strain of 1% in the linear viscoelastic region was selected when the angular frequency was varied to obtain the dynamic viscoelastic properties. (B) Rheological angular frequency change test results of hydrogels with different compositions. (C) The viscoelastic stability of the PEMN hydrogel characterized by rheology.

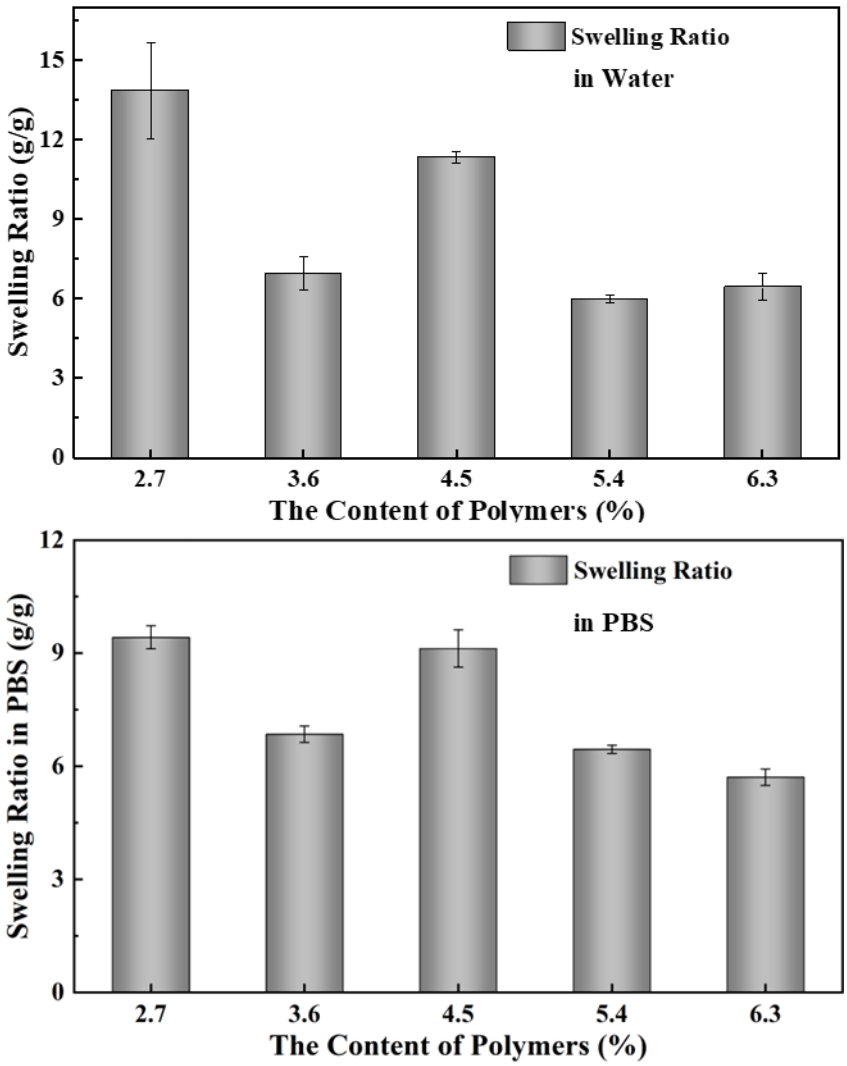

Fig. S8. Swelling ratio of hydrogels of different compositions in water or in PBS.

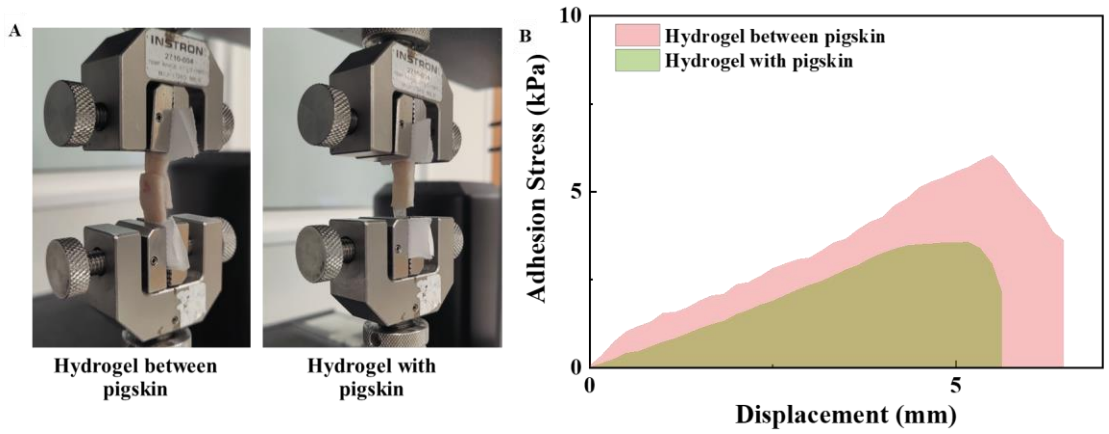

Fig. S9. (A) The images of the adhesion test of PEMN hydrogels; (B) The adhesion curve of the adhesion test of PEMN hydrogels. The adhesion stress of the hydrogel directly adhered in the middle of the pigskin or the samples composed of the hydrogel and pigskin was 6.07 ± 0.05 kPa and 2.69 ± 0.77 kPa, respectively, demonstrating the possibility of adhesion of the hydrogel *in-vivo*, but the adhesion was inferior to the samples that have undergone a sol-gel transition on the pigskin, which may arise from the formation of a relatively strong bond between the solid-liquid states when the sol state was applied to the pigskin compared to the solid-solid states when the hydrogel was directly applied to the pigskin and a greater cohesion force compared to the adhesion force after acidification double-effect post-enhancing process.

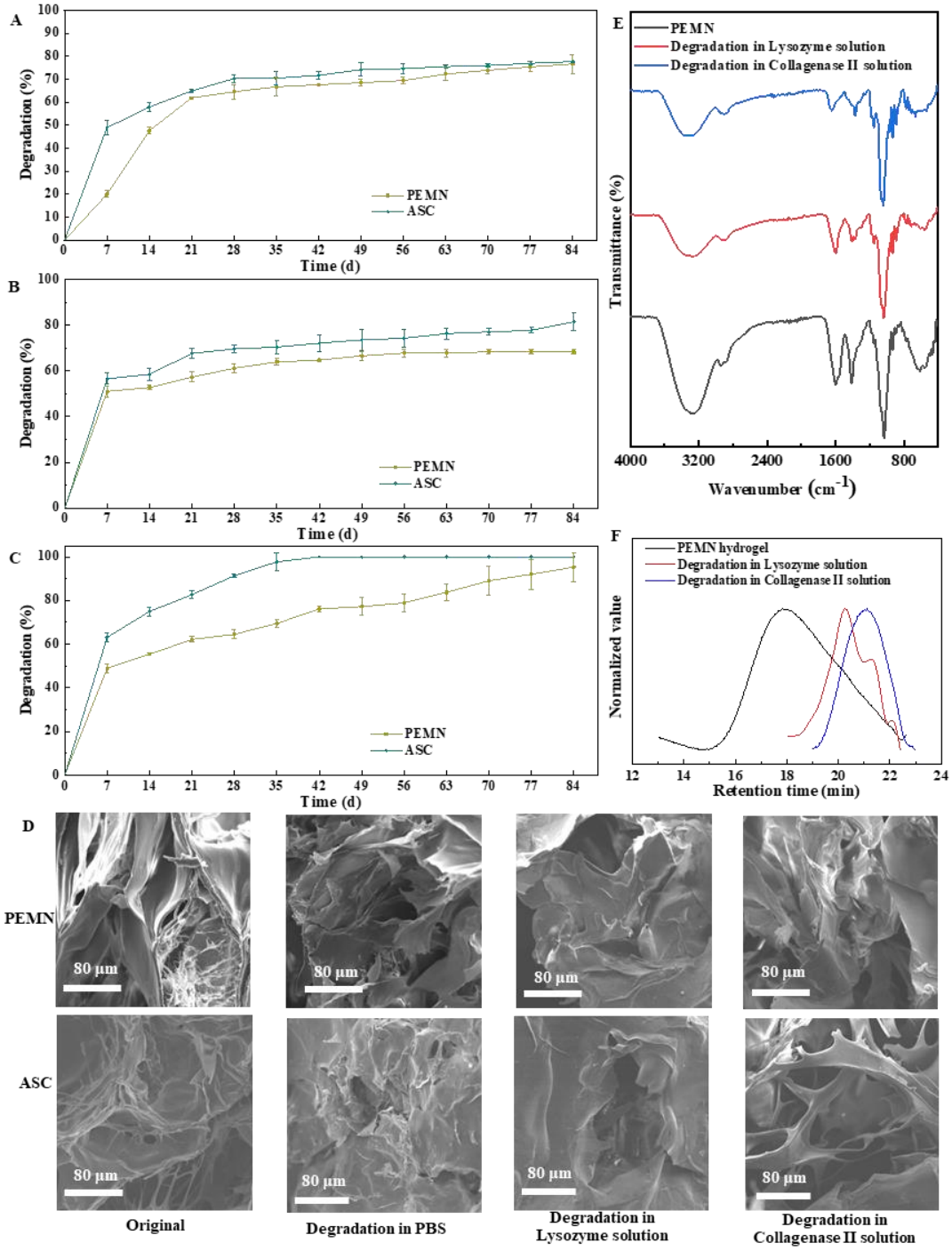

Fig. S10. Degradation curve of PEMN and ASC hydrogels in (A) PBS, (B) Lysozyme, (C) collagenase II solution. (D) Morphology of PEMN and ASC hydrogels before and after degradation. (E) FTIR spectrum and (F) normalized GPC curve of PEMN hydrogels before and after degradation. According to the ATR-FTIR spectrum, the hydrogen bond strength of the hydrogels after degradation decreased significantly and the number of methyl groups increased, indicating the destruction of the cross-linked structure and the breakage of molecular chains. The GPC test results showed that compared with the M_w of the original sample (M_w = 14822), the M_w of the hydrogel after 12 weeks of degradation by lysozyme and collagenase II solutions were 150 and 105, respectively, which further verified the degradability of the PEMN hydrogel.

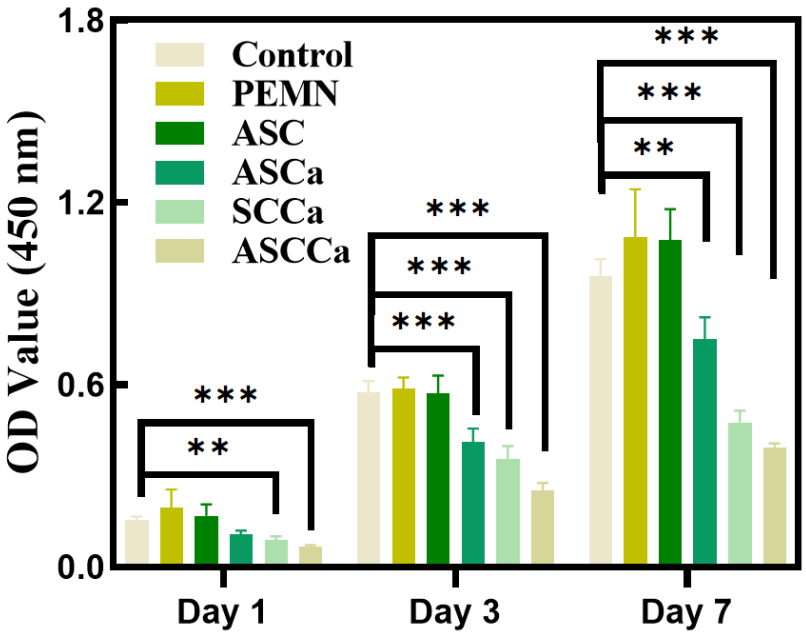

Fig. S11. CCK-8 assay results of rBMSCs cocultured with different leaching solutions for 1, 3 and 7 days. The extract is made of 50 mg wet hydrogel in 1 mL α-MEM soaked for 24h.

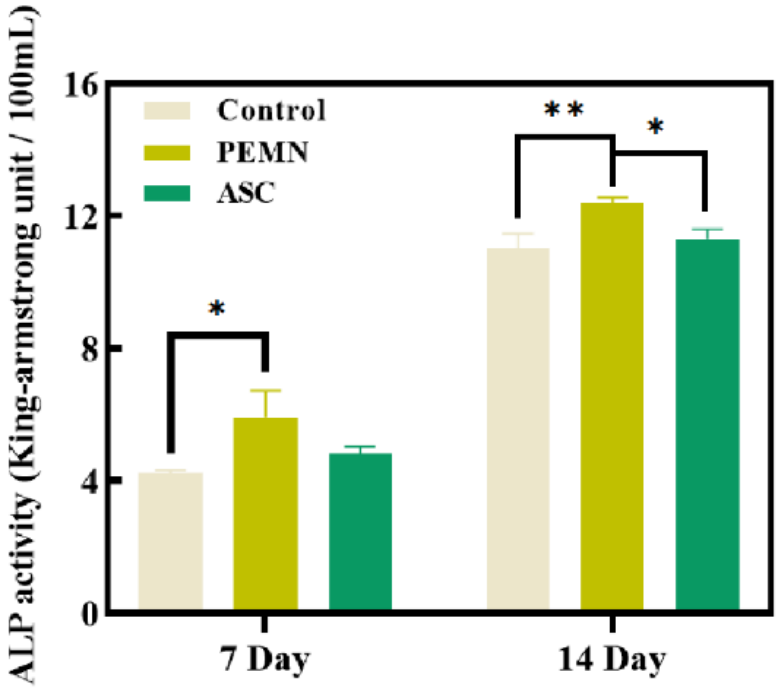

Fig. S12. Expression of ALP activity of BMSCs co-cultured with different hydrogel scaffolds for 7 days and 14 days.

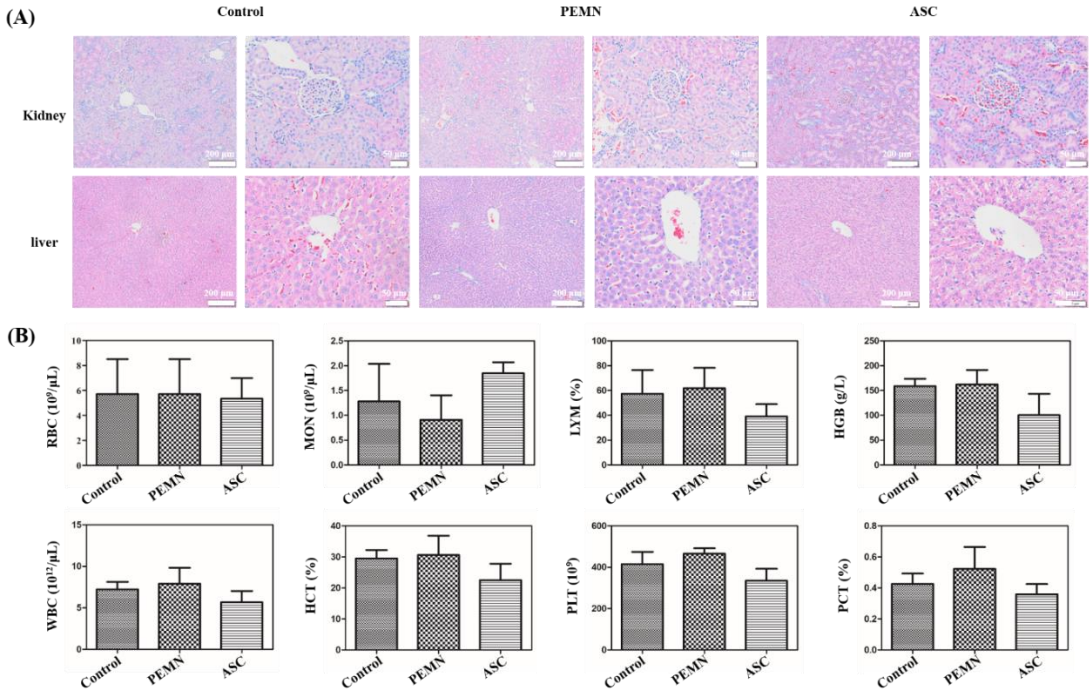

Fig. S13. *In vivo* toxicity evaluation of PEMN and ASC hydrogels. (A) H&E staining of kidney and liver. (B) Blood biochemical indexes of animals in the blank control group, PEMN hydrogel group, and ASC hydrogel group. Data were presented as mean ±SD, n=3, ** $P < 0.01$ and * $P < 0.05$, and analyzed by ANOVA.

Table S1. The original components of different hydrogels, in which the proportion is the percentage of the weight of natural polymers in the total weight of the system.

Hydrogel Type	*m(Agar)* (g)	*m(SA)* (g)	*m(CTS)* (g)	*m($CaCO_3$)* (g)	*V(Water)* (mL)	*m(Glycerin)* (g)	Methods
PEMN-2.7%	0.23	0.28	0.17	0.16			PFDEPE
PEMN-3.6%	0.23	0.43	0.26	0.24			PFDEPE
PEMN-4.5%	0.23	0.58	0.35	0.32			PFDEPE
PEMN-5.4%	0.23	0.73	0.44	0.4			PFDEPE
PEMN-6.3%	0.23	0.88	0.53	0.48	23	1	PFDEPE
ASC	0.23	0.28	0.17	0			PFDEPE
ASCa	0.23	0.28	0	0.16			PFDEPE
SCCa	0	0.28	0.17	0.16			SD-A-SGT
ASCCa	0.23	0.28	0.17	0.16			SD-A-SGT

Table S2. Gelation time of preforming hydrogels with different components.

Hydrogel Type	Hydrogel preforming time
Preformed PEMN-2.7%	87.72s
Preformed PEMN-3.6%	79.30s
Preformed PEMN-4.5%	67.39s
Preformed PEMN-5.4%	62.24s
Preformed PEMN-6.3%	38.37s
Agar	170.18s

Table S3. Elastic modulus of hydrogels with different components.

Hydrogel Type	Tensile elastic modulus (kPa)	R^2	Compression elastic modulus (kPa)	R^2
PEMN-2.7%	390.71	0.993	160.99	0.974
PEMN-3.6%	445.08	0.992	327.03	0.988
PEMN-4.5%	523.24	0.988	447.56	0.997
PEMN-5.4%	612.12	0.992	561.25	0.998
PEMN-6.3%	640.33	0.996	643.64	0.998
ASC	71.14	0.979	7.91	0.932
ASCa	121.77	0.987	97.36	0.973
SCCa	232	0.976	35.55	0.963
ASCCa	289.96	0.987	141.89	0.991

S3 Discussion

The choice of these three kinds of polymers was based on their functions. Each polymer in our study serves a specific purpose.

Agar is utilized for its temperature-sensitive sol-gel transition reversibility, enabling the preparation of preformed hydrogels. Agarose gel, the main component of agar, has been reported as a supportive material for chondrogenesis of human bone marrow-derived mesenchymal stem cells, indicating its potential in cartilage regeneration.[2,3] Moreover, agar-based hydrogels exhibit durable adhesive effects attributed to the presence of abundant hydrogen bonds.[4] Besides, owing to the temperature-sensitive property, the sol can be cast into a mold or extruded through a syringe and such a controllable fabrication process is convenient for the adjustment of the preparation steps and ingredients.

Alginate and chitosan were selected as the formation of the hierarchical chain entanglements to further promise the simultaneous achievement of shape controllability and high toughness. Alginate is commonly employed in osteochondral repair and tissue engineering scaffolds due to its favorable biocompatibility and hydrophilicity.[5,6] At the same time, alginate was used for the physical cross-linking network in the double network hydrogel because of its easy-to-achieve cross-linking method and high mechanical strength of the unzipped ionic crosslinks.[7] In this work, the enhanced mechanical strength was achieved due to the ionic crosslinking between Ca^{2+} and SA, and the electrostatic interaction between the protonated amino groups of CTS and the negatively charged carboxyl groups of SA. Chitosan exhibits excellent biocompatibility, low toxicity, and immunostimulatory activities. It can be enzymatically degraded by lysozyme and chitosanase enzymes *in vivo*.[5] Chitosan has shown potential in cartilage and bone tissue engineering by promoting the expression of extracellular matrix (ECM) proteins in chondrocytes and osteoblasts, as well as inducing intramembranous bone formation and vascularization.[8] In addition, as the only alkaline polysaccharide existing in nature, chitosan can form the high-strength physical hydrogel through electrostatic interaction with sodium alginate.[9]

In general, in this work, the achievement of the controllability and high toughness of PEMN hydrogel was attributed to the hierarchical chain entanglements consisting of the hydrogen bonding of agar, electrostatic interaction between CTS and SA, and ionic crosslinking between SA and Ca^{2+}. Therefore, these polymers are irreplaceable in achieving shape controllability and high toughness by such a PFDEPE method for efficient osteochondral regeneration. However, for other applications, we consider PFDEPE as a versatile

method where agar components in preformed gels can be substituted with thermoreversible polymers like carrageenan or gellan gum. Similarly, the components used for mechanical reinforcement can be replaced with other tough natural or synthetic polymer networks, such as carboxymethyl chitosan or acrylamide.

References

1. Y. B. Ji, S. Lee, H. J. Ju, H. E. Kim, J. H. Noh, S. Choi, K. Park, H. B. Lee and M. S. Kim, *J. Control. Release*, 2023, **356**, 43–58.
2. T. A. S. Selmi, P. Verdonk, P. Chambat, F. Dubrana, J. Potel, L. Barnouin and P. Neyret, *J. Bone Joint Surg. [Br]*, 2008, **90-B**, 597-604.
3. C. Y. Huang, P. M. Reuben, G. D'Ippolito, P. C. Schiller and H. S. Cheung, *Anat. Rec.*, 2004, **278A**, 428–436.
4. D. Zhang, F. Yang, J. He, L. Xu, T. Wang, Z. Feng, Y. Chang, X. Gong, G. Zhang and J. Zheng, *ACS Appl. Polym. Mater.*, 2020, **2**, 1031–1042.
5. Y. Li, J. Rodrigues and H. Tomas, *Chem. Soc. Rev.*, 2012, **41**, 2193-2221.
6. Y. Chen, Y. Chen, X. Xiong, R. Cui, G. Zhang, C. Wang, D. Xiao, S. Qu and J. Weng, Mater Today Bio, 2022, 14, 100261.
7. J. Sun, X. Zhao, W. R. K. Illeperuma, O. Chaudhuri, K. H. Oh, D. J. Mooney, J. J. Vlassak and Z. Suo, *Nature*, 2012, **489**, 133-136.
8. J. Fang, J. Liao, C. Zhong, X. Lu and F. Ren, *ACS Biomater. Sci. Eng.*, 2022, **8**, 4449–4461.
9. S. Tang, J. Yang, L. Lin, K. Peng, Y. Chen, S. Jin and W. Yao, *Chem. Eng. J.*, 2020, **393**, 124728.